Journal of Catalysis **200,** 203–208 (2001)
doi:10.1006/jcat.2001.3197, available online at http://www.idealibrary.com on IDEAL®

Mechanism of O_2 Desorption during N_2O Decomposition on an Oxidized Rh/USY Catalyst

Shin-ichi Tanaka, Koichi Yuzaki, Shin-ichi Ito, Satoshi Kameoka, and Kimio Kunimori[1]

Institute of Materials Science, University of Tsukuba, Tsukuba, Ibaraki 305-8573, Japan

Received July 10, 2000; revised February 6, 2001; accepted February 6, 2001; published online April 24, 2001

Pulsed N_2O decomposition on a reduced or oxidized Rh/USY catalyst has been carried out to study the dependence of oxygen coverage (θ_o) on activity and to study the mechanism of O_2 desorption using an isotopic tracer technique. Decomposition activity decreased to the minimum (formation of only N_2) at $\theta_o = 0.5$, but increased with increasing coverage ($\theta_o > 0.5$), and finally high activity with steady-state O_2 production was attained at high θ_o (>1.2). In the isotope study, N_2 ^{16}O was pulsed onto ^{18}O/oxidized Rh catalyst at low temperatures (220–240°C), and desorbed O_2 molecules were monitored by means of mass spectrometry. The ^{18}O fraction in the desorbed oxygen had almost the same value as that on the surface oxygen. The result shows that O_2 desorption does not proceed via the Eley–Rideal mechanism, but via the Langmuir–Hinshelwood mechanism, i.e., desorption of dioxygen through the recombination of adsorbed oxygen. On the other hand, O_2-TPD measurements in He showed that desorption of oxygen from the Rh catalyst occurred at much higher temperatures. Therefore, it was proposed that reaction-assisted desorption of O_2 occurs during N_2O decomposition at low temperatures.

Key Words: **N_2O decomposition; ^{18}O isotope; Rh/USY catalyst; mechanism of O_2 desorption; oxygen coverage; temperature-programmed desorption.**

INTRODUCTION

Nitrous oxide (N_2O), which has been considered a strong greenhouse gas, also contributes to catalytic stratospheric ozone destruction (1). Therefore, the catalytic decomposition of N_2O ($N_2O \rightarrow N_2 + \frac{1}{2}O_2$) has been attracting much attention (1–10). Various research groups have studied supported noble or transition metal catalysts (2–5) and oxides (6, 7) for N_2O decomposition at different temperatures (250–500°C). We have reported that a Rh/USY catalyst was very active for the catalytic decomposition of N_2O even at low temperatures around 250°C ($SV = 60{,}000\ h^{-1}$) (8). A pulsed N_2O experiment over the Rh/USY catalyst (at 260°C) showed that only N_2 was produced on a reduced Rh surface, but O_2 production started on an oxygen-covered Rh surface (9). Furthermore, an O_2-TPD measurement (in He) showed that O_2 was not desorbed up to 600°C (9). In practice, TPD experiments (*in vacuo*) show that oxygen atoms on a Rh(111) surface desorb to form O_2 at 800°C (11). Therefore, why O_2 is desorbed at such low temperatures during catalytic N_2O decomposition over Rh/USY catalyst remains an open question.

The mechanisms of N_2O decomposition have been given as follows (1, 10):

$$N_2O \rightarrow N_2 + O(a), \quad [1]$$

$$2O(a) \rightarrow O_2, \quad [2]$$

$$N_2O + O(a) \rightarrow N_2 + O_2. \quad [3]$$

Step [1] is dissociative N_2O adsorption followed by the production of N_2 and adsorbed oxygen on the catalyst surface. Step [2] is O_2 desorption by the recombinative desorption of adsorbed oxygen, and the so-called Langmuir–Hinshelwood (LH) mechanism is described by steps [1] and [2]. As stated above, however, it may be difficult to expect that step [2] prevails at low temperatures. Step [3] is oxygen removal via the Eley–Rideal (ER) mechanism (4), which might be possible at relatively low reaction temperatures (4, 12). In the case of the Rh/USY catalyst described above (9), it appeared that O_2 is freed on collision of N_2O with the adsorbed oxygen (step [3], ER mechanism). Dandl and Emig (12) proposed a mechanistic model from the kinetics simulation, where the ER mechanism prevails at lower temperatures and the LH mechanism prevails at higher temperatures. On the other hand, the hot-atom (HA) mechanism (13) may also be considered, where only hot (nascent) O(a) atoms produced by step [1] are desorbed via step [2].

We have already studied the mechanism of N_2O decomposition on an oxidized Rh black catalyst (without the support) using an ^{18}O tracer technique (i.e., using N_2 ^{16}O pulse onto ^{18}O(a)-covered Rh surface) (14). Surprisingly, the O_2 desorption was found to proceed via step [2] (i.e., LH mechanism) at 220°C, and O_2-TPD (in He) showed that desorption of oxygen occurred at higher temperatures (14). Because the recombinative desorption of oxygen did not occur in He at 220°C, we have proposed reaction-assisted

[1] To whom correspondence should be addressed. E-mail: kunimori@ims.tsukuba.ac.jp. Fax: +81-298-55-7440.

0021-9517/01 $35.00

desorption of O_2 during N_2O decomposition at low temperature (14).

In this work, the ^{18}O tracer technique was applied to the Rh/USY catalyst to elucidate the mechanism of O_2 desorption. It is of interest to make clear whether LH-type recombinative desorption of oxygen (i.e., step [2]) also prevails or not on the supported Rh catalyst. Before the isotopic study, pulsed N_2O experiments were carried out to study the oxygen coverage dependence on activity (N_2 and O_2 formation), and O_2-TPD studies were also performed to elucidate the nature of the adsorbed oxygen.

EXPERIMENTAL

A Rh/USY catalyst was prepared by incipient wetness impregnation of USY (TOSOH Co., $Si/Al_2 = 14.6$) with an aqueous solution of $Rh(NO_3)_3$ followed by calcination in air at 600°C for 3 h (9). The Rh loading on USY was 2 wt%. H_2 and CO chemisorption measurements were performed with a conventional volumetric adsorption apparatus (15, 16). Total adsorption of H_2 (H/Rh), as well as irreversible adsorption of CO (CO/Rh), was measured after H_2 reduction for 1 h at 500°C. In this work, for the Rh/USY catalyst, H/Rh and CO/Rh were 0.54 and 0.51, respectively.

The reaction of N_2O decomposition was performed in a microcatalytic pulse reactor (9, 14). A quartz tube reactor (i.d. 4 mm) was charged with 19.5 mg of the Rh/USY catalyst (5 mm in height, Rh = 3.79 μmol), and it was treated in H_2 reduction for 1 h at 500°C before measurement. Highly purified He (99.9999%) was used as a carrier gas at a flow rate of 55 cm^3/min. A pulse of 0.517% N_2O in He (0.27 μmol/pulse) was injected by a jacketed switching valve purged with He. No decomposition was observed on the USY support only, even at 500°C.

Isotope-labeled $^{18}O_2$ (96.5% $^{18}O_2$) was obtained from Icon Company Ltd. The ^{18}O tracer-loaded catalyst was prepared as follows: the catalyst was treated with $^{18}O_2$ (80 Torr) in an *in situ* closed system at 300°C for 3 h after H_2 reduction at 500°C. The reactant gas (0.517% N_2 ^{16}O in He) and probe gases (0.208% $^{18}O_2$ in He and 0.103% $C^{16}O$ in He) were flushed onto the catalyst via the carrier gas. The amount of N_2O was 0.27 μmol/pulse, $^{18}O_2$ 0.10 μmol/pulse, and CO 0.04 μmol/pulse. The effluent was analyzed in an on-line gas chromatograph system equipped with a TCD detector (Shimadzu, GC-8A) and differentially pumped quadrupole mass spectrometer (Balzers, QMS 200 F). To prevent leakage of $^{16}O_2$ from the atmosphere into the gas line, the whole apparatus, which was located in a corner of the laboratory room, was isolated from the atmosphere by drawing curtains to make a small room in which N_2 gas was purged.

Quantitative TPD measurement in a He flow was performed using 19.5 mg of the Rh/USY catalyst (3.79 μmol as Rh metal). The analysis equipment used was the same as for the isotopic tracer study. The temperature was increased from room temperature to 800°C at a constant heating rate of 10°C/min and was kept at 800°C for 20 min.

RESULTS AND DISCUSSION

Dependence of Oxygen Coverage on N_2O Decomposition

N_2O pulses were injected onto the Rh/USY catalyst after H_2 reduction at 500°C. Figure 1 shows amounts of products (N_2 and O_2) from N_2O decomposition at 260°C to each pulse (0.517% N_2O in He). The pulse interval was 3 min. Until the 19th pulse, the product was only N_2 . The amount was 0.27 μmol (equivalent to 100% conversion of N_2O) for the first pulse, and it decreased until the 9th pulse. After the 10th pulse it increased slowly, and finally reached a stable state. On the other hand, O_2 was produced after the 19th pulse, and the amount also increased slowly, finally reaching a stable state. Because no O_2 was desorbed until the 19th pulse, the amount of adsorbed oxygen (i.e., oxygen coverage) was increased with pulsing N_2O (step [1]). Here, the coverage of oxygen (θ_o) was defined as the atomic ratio of the number of adsorbed oxygens to the number of surface rhodiums (Rh_s), which was based on the H/Rh value (0.54). The θ_o at each stage can be easily calculated from the data in Fig. 1. Figure 2 shows the activity of N_2O decomposition as a function of θ_o on the Rh/USY catalyst at 220 and 260°C, respectively. A drastic decrease in N_2O conversion was observed with increasing θ_o (up to 0.5), which may be consistent with the literature (17). In practice, according to the study on the sticking coefficient of N_2O on Rh(110) (17), the dissociative chemisorption of N_2O (step [1]) stops at $\theta_o = 0.5$. Note that in the case of single-crystal work, exposure of the sample to N_2O gas was orders of magnitude

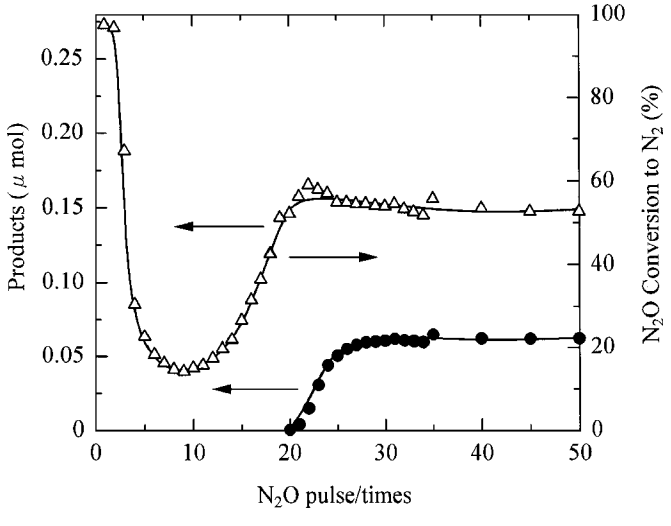

FIG. 1. Amount of products from each pulse of N_2O over the Rh/USY catalyst at 260°C: (△) N_2, (●) O_2.

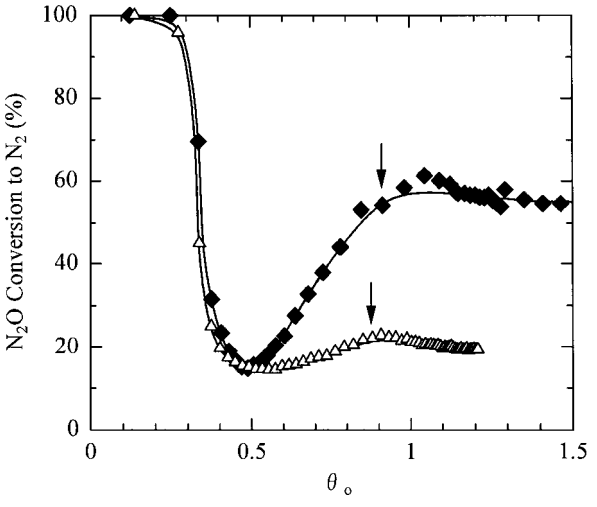

FIG. 2. Conversion of N_2O to N_2 over the Rh/USY catalyst as a function of oxygen coverage: (△), 220°C; (◆), 260°C. O_2 formation started at $\theta_o \fallingdotseq 0.9$ (indicated by the vertical arrows).

lower. In the case of supported Rh (see Fig. 2), an increase in activity was observed with increasing θ_o (>0.5), O_2 production started at $\theta_o \fallingdotseq 0.9$, and finally, steady-state activity was attained at high θ_o (>1.2). This phenomenon appears not to be related to a diffusion process such as oxygen spillover from Rh particles to the support, because the same results as in Figs. 1 and 2 were obtained when the pulse interval was changed to 9 min. The adsorbed oxygen species with high θ_o may play an important role in the formation of active sites for O_2 production.

It should be noted here that the N_2/O_2 ratio was 2.0 at steady state in the flow reactor system (8, 9). In Fig. 1, however, the N_2/O_2 ratio was 2.4 at the 50th pulse. This means that oxygen was still adsorbed on the Rh surface even after the 50th pulse ($\theta_o = 1.5$), and the adsorbed oxygen may be located in the subsurface layer. On the other hand, after a N_2O flow treatment (0.517% N_2O in He) at 220 or 260°C for 1 h, the N_2/O_2 ratio was constant (2.0) from the 1st N_2O pulse.

O_2-TPD Studies on N_2O- or O_2-Treated Rh Catalyst

To elucidate the difference in the states of the adsorbed oxygen species, O_2-TPD spectra were measured at different θ_o after N_2O or O_2 pretreatments. Figure 3 shows O_2-TPD spectra from the catalyst after H_2 reduction at 500°C followed by N_2O pretreatments (A, B, or C) at 220°C. In the case of pretreatments A and B using N_2O pulses, oxygen coverage can be calculated from the data in Fig. 1, as shown in the inset to Fig. 3 ($\theta_o = 0.5$ after 10 N_2O pulses and $\theta_o = 1.2$ after 50 N_2O pulses). It should be recalled that the minimum and steady-state activities were observed after the pretreatments A and B, respectively (Fig. 2). As shown in Fig. 3, O_2 desorption starts at 700°C after pretreatment A, whereas it starts at 550°C after pretreatment B. The amount of desorbed O_2 (atomic O/Rh_s) was (A) 0.23 and (B) 0.85, respectively, which are significantly lower than the dosed values ($\theta_o = 0.5$ and 1.2, respectively). This result suggests that a large amount of oxygen was not desorbed when the temperature was kept at 800°C for 20 min. After the N_2O flow, pretreatment C, the O_2-TPD peak was similar to that after pretreatment B, although the peak area was larger ($O/Rh_s = 0.98$) after the N_2O flow than after the N_2O pulses. The results in Fig. 3 suggest that oxygen species with weaker O–Rh bonds, which are desorbed below 700°C in the O_2-TPD experiment, play an important role in the high activity as well as steady-state O_2 production in the catalytic N_2O decomposition.

Similar TPD experiments were also performed using O_2 pulses to elucidate the differences in the states of adsorbed oxygen. Figure 4 shows O_2-TPD spectra from the Rh/USY catalyst after H_2 reduction at 500°C followed by the pretreatments using O_2 pulses (A and B) at 220°C. As shown in the inset to Fig. 4, θ_o was 0.5 after 5 O_2 pulses, pretreatment A, and 1.0 after 25 O_2 pulses, pretreatment B. The amount of desorbed O_2 (O/Rh_s) was (A) 0.55 and (B) 0.89, respectively, which are roughly consistent with the dosed values ($\theta_o = 0.5$ and 1.0, respectively). Therefore, it is suggested that N_2O pretreatments leads to the formation of stronger O–Rh bonds than O_2 pretreatments, in particular at low θ_o (=0.5). At high θ_o (≥1.0), however, both N_2O and O_2 pretreatments gave oxygen species with weaker O–Rh bonds, which were desorbed below 700°C.

In Fig. 2, it is not clear at the present stage why N_2O conversion increases at higher θ_o coverages. From the HREEL study of oxygen structures on Rh(110), the Rh surface was reconstructed with increasing θ_o, and the structural

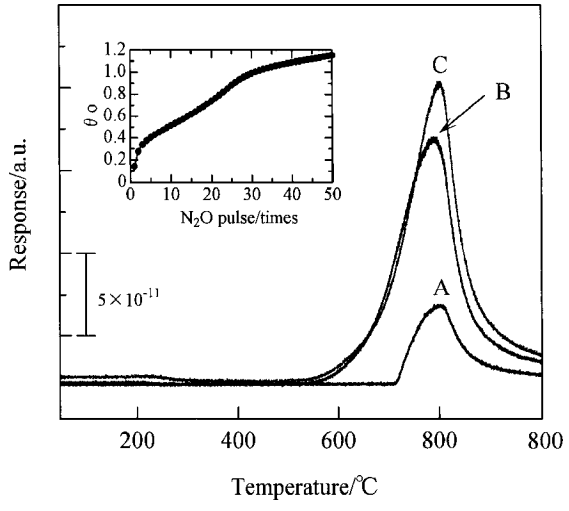

FIG. 3. Temperature-programmed desorption (TPD) spectra of O_2 from the Rh/USY catalyst after N_2O pretreatments: Pretreatment A: 0.517% N_2O in He (10 pulses at 220°C). Pretreatment B: 0.517% N_2O in He (50 pulses at 220°C). Pretreatment C: 0.517% N_2O in He (flow, 30 ml/min for 1 h at 220°C).

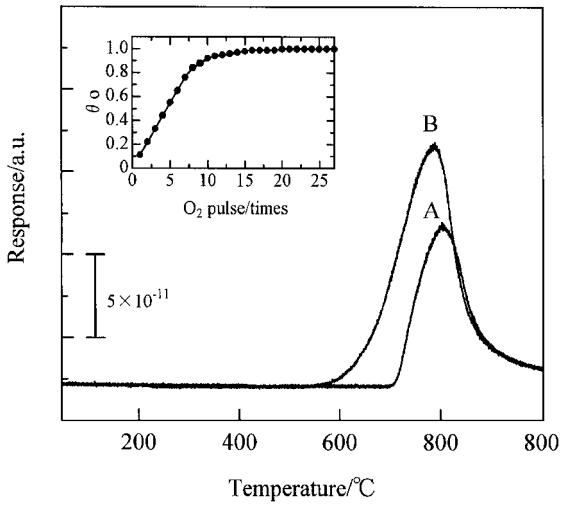

FIG. 4. Temperature-programmed desorption (TPD) spectra of O_2 from the Rh/USY catalyst after O_2 pretreatments: Pretreatment A: 0.208% O_2 in He (5 pulses at 220°C). Pretreatment B: 0.208% O_2 in He (25 pulses at 220°C).

changes led to the formation of different oxygen species (18). Changes in the surface structures with weaker O–Rh bonds may result in the high activity as well as steady-state O_2 production, although this is a subject for future work.

Figure 5 shows the O_2-TPD spectrum from the Rh/USY catalyst after H_2 reduction at 500°C followed by O_2 treatment (80 Torr) at 300°C, which was the same as used in the isotope study. The spectrum is similar in shape to spectra B and C in Fig. 3 and spectrum B in Fig. 4. Oxygen coverage (θ_o) was determined to be 1.1 from the amount of desorbed oxygen (O/Rh_s). It should be noted that no O_2 desorption takes place below 500°C.

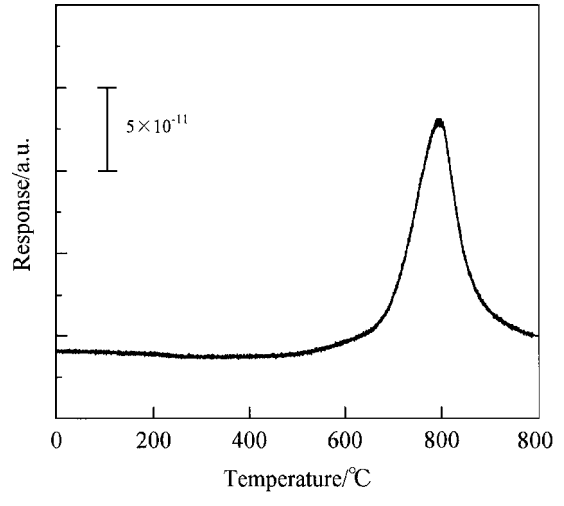

FIG. 5. Temperature-programmed desorption (TPD) spectrum of O_2 from the Rh/USY catalyst after O_2 (80 Torr) pretreatment at 300°C.

Mechanism of O_2 Desorption Using Isotopic Tracer Technique

The reduced Rh/USY catalyst was oxidized with $^{18}O_2$ (96.5%) gas at 300°C, and pulsed N_2O decomposition was carried out at 220°C. An isotopic equilibrium constant, K_e, should be considered to judge incidental exchange reactions that would disguise the experimental results. Taking into account an equilibrium reaction,

$$^{18}O_2 + {}^{16}O_2 \rightleftarrows 2\,{}^{18}O{}^{16}O, \qquad [4]$$

K_e is generally given as

$$K_e = \frac{[{}^{18}O{}^{16}O]^2}{[{}^{18}O_2][{}^{16}O_2]}. \qquad [5]$$

If the exchange reaction equilibrates, K_e should be close to 4 (19). The same rule applies for other exchange reactions. An isotopic fraction of $^{18}O[{}^{18}f = {}^{18}O/({}^{16}O + {}^{18}O]$ on the Rh surface can be evaluated by a pulsed $C^{16}O$ experiment. It should be noted that the amount of CO pulse (0.04 μmol) is negligible compared with that of surface Rh atoms (2.05 μmol), which was estimated by H_2 chemisorption (H/Rh). Table 1 shows the ${}^{18}f$ and K_e for the product molecules obtained at 220°C. The CO molecules react with the surface oxygen to form CO_2, and CO conversion was 100% in the pulse experiment at 220°C. The exchange reaction of oxygen in CO_2 is fast on metals (19). As shown in Table 1, K_e is 4.00, which suggests that the isotopic exchange of oxygen in CO_2 equilibrates (Table 1, Expt. 1). Therefore, the ${}^{18}f$ in the product CO_2 should be equal to that of the surface oxygen. Since ${}^{18}f$ in the product CO_2 was 0.69 (Table 1, Expt. 1), the ${}^{18}f$ on the Rh surface after $^{18}O_2$ treatment was determined to be 0.69. As a separate experiment, the $^{18}O_2$ pulse was injected onto ^{16}O-covered catalyst at 220°C (Table 1, Expt. 3). Comparing the ${}^{18}f$ value measured without the Rh/USY catalyst (0.94; Table 1, Expt. 4) with 0.68,

TABLE 1

Isotopic Fraction ^{18}O (${}^{18}f$) and Isotopic Equilibrium constant (K_e) in the Product Molecules from $^{18}O_2$, $C^{16}O$, and $N_2\,{}^{16}O$ Pulses at 220°C

Experiment	Pulse	Surface species	Product	${}^{18}f$	K_e
1	$C^{16}O$	^{18}O	CO_2	0.69	4.00
2	$N_2\,{}^{16}O$	^{18}O	O_2	0.62	1.97
2	$N_2\,{}^{16}O$	^{18}O	N_2O	0.00[a]	—
3	$^{18}O_2$	^{16}O	O_2	0.68	0.37
4	$^{18}O_2$	—	O_2	0.94[b]	—

[a] The isotopic abundance of ^{18}O is 0.002.
[b] ${}^{18}f$ in the incident pulse measured without the catalyst.

the exchange coefficient of O_2 (C) with surface oxygen,

$$^{18}O_2 + {}^{16}O(a) \rightarrow {}^{18}O{}^{16}O + {}^{18}O(a), \quad [6]$$

$$^{16}O_2 + {}^{18}O(a) \rightarrow {}^{18}O{}^{16}O + {}^{16}O(a), \quad [6']$$

was estimated to be 0.28. The exchange coefficient (C) represents the isotope fraction produced during a single pass of O_2 exchanging with the surface oxygen.

After the pulsed CO experiment, an N_2 ^{16}O pulse was injected onto the catalyst at 220°C (Table 1, Expt. 2). N_2O conversion was about 15%, and the ^{18}f of the product O_2 was 0.62, which was almost the same as the ^{18}f of the Rh surface. In addition, the K_e value of oxygen produced from N_2O decomposition was 1.97, which indicates that the exchange of oxygen between gas phase and surface is slow enough at low reaction temperature (220°C). Furthermore, the exchange of oxygen in N_2O with surface oxygen,

$$N_2\,{}^{16}O + {}^{18}O(a) \rightarrow N_2\,{}^{18}O + {}^{16}O(a), \quad [7]$$

can be neglected because of the very low ^{18}f value in the outlet N_2O (Table 1, Experiment 2).

The mechanism of oxygen desorption is determined by the following discussion. The ^{18}O fraction of the product O_2 ($^{18}f_{\text{calc.}}$) can be calculated based on the three mechanisms (LH, ER, and HA). However, the $^{18}f_{\text{calc.}}$ of the outlet O_2 should be corrected for O_2 exchange reactions using the exchange coefficient (C), as follows:

$$^{18}f_{\text{calc.}} = A(1 - C) + BC. \quad [8]$$

Here, A is the ^{18}O fraction of the product O_2 just desorbed from the catalyst surface, and B is the ^{18}O fraction of the surface (i.e., $B = 0.69$; Table 1, Expt. 1). In Eq. [8], BC represents the ^{18}O fraction in the product O_2 coming from the surface, while $A(1 - C)$ represents the product O_2 without going to the surface. Table 2 shows the observed ^{18}f of the product O_2 produced from N_2O decomposition and the calculated ^{18}f values based on the three mechanisms (LH, ER, and HA). In the case of the LH mechanism ($2O(a) \rightarrow O_2$, i.e., step [2]), the $^{18}f_{\text{calc.}}$ of the product oxygen should be the same as that of the surface oxygen (i.e., 0.69). Even though incidental exchange reactions between the product O_2 and the O(a) (i.e., steps [6] and [6′]) occur, $^{18}f_{\text{calc.}}$ does not change: ^{18}O fractions coming from the surface and going to the surface by the exchange reaction are canceled (i.e., BC in Table 2), because $A = B$ in the case of the LH mechanism. As shown in Table 2, the experimental result is in good agreement with the LH mechanism. In the case of the ER mechanism (i.e., step [3]), the ^{18}O fraction of the product O_2 should be half the value of the surface oxygen (i.e., 0.345). However, considering the exchange coefficient ($C = 0.28$), the $^{18}f_{\text{calc.}}$ of the product O_2 becomes 0.44 (Table 2), which is quite different from the observed ^{18}f. Therefore, the ER mechanism can be excluded. It should be noted that the product O_2 is formed during contact with the catalyst during N_2O reaction, whereas the C value is measured by reaction with just the O_2 pulse. This presumably means that, since O_2 is produced during the reaction, the C value should be corrected for the fact that O_2 is not present in the catalyst bed the whole time, and presumably be reduced by a factor of 2 (i.e., $C = 0.14$). This leads to a corrected $^{18}f_{\text{calc.}}$ value for the ER mechanism of 0.39, which is more different from the observed $^{18}f_{\text{calc.}}$ value. The HA mechanism, which produces O_2 molecules only from N_2 ^{16}O, can also be excluded. In this case, $^{18}f_{\text{calc.}}$ is 0.19 (Table 2) by considering only step [6′], because the $^{16}O_2$ that is formed can react with adsorbed ^{18}O. If the corrected C value (0.14) is used, the $^{18}f_{\text{calc.}}$ value becomes 0.10, which is quite different from the observed ^{18}f value. If the "hot" oxygen can react with all adsorbed oxygen atoms, $^{18}f_{\text{calc.}}$ takes the same value as in the ER mechanism. Therefore, the present result reveals that oxygen desorption proceeds via the LH mechanism (i.e., recombinative desorption of O_2).

TABLE 2

Observed ^{18}f and Calculated ^{18}f Values Based on the Three Mechanisms

Mechanism	^{18}f of O_2 just produced	Equation	$^{18}f_{\text{calc.}}$ $C = 0.28$	$^{18}f_{\text{calc.}}$ $C = 0.14$
LH	$A = B$	$B(1 - C) + BC$	0.69	0.69
ER	$A = 1/2B$	$1/2B(1 - C) + BC$	0.44	0.39
HA	$A = 0$	BC	0.19	0.10
Observed			$^{18}f_{\text{obs.}} = 0.62$	

The LH mechanism was also supported at a reaction temperature of 240°C. It should be noted that the oxygen exchange coefficient (C) increased with reaction temperature ($C = 0.34$ at 240°C, $C = 0.71$ at 300°C), while oxygen exchange with the USY support was negligible ($C = 0.05$ even at 500°C). The isotopic experiments were possible only in a relatively narrow range of temperatures, because at higher temperatures (e.g., 300°C) K_e was 4.0 due to the high C value, while at lower temperatures N_2O conversions were too low to obtain reliable results. As mentioned in the Introduction, the LH mechanism (i.e., recombinative desorption of O_2) was also observed on unsupported Rh catalyst. At present there appears to be no dependence of the support on the reaction mechanism, because similar results have been obtained for a Rh/SiO_2 catalyst (20).

In the present study, all of the surface oxygens are involved in the recombinative desorption of O_2 (step [2]) at low reaction temperatures (220–240°C). The TPD study in Fig. 5 shows that desorption of O_2 in He from the Rh/USY catalyst does not take place at these temperatures. Therefore, it should be considered that the energy of O–Rh bond

formation accompanied by N_2O decomposition may transfer to the surrounding adsorbed oxygen atoms on the Rh surface; i.e., step [2] ($2O(a) \rightarrow O_2$) proceeds via reaction-assisted desorption, as previously proposed in the case of the Rh black catalyst (14). In practice, a large bonding energy has been reported for O–Rh (96.8 kcal/mol) (21) and additional energy is released by formation of an N≡N bond (17). These exothermic processes can overcome the energy loss caused by breakage of the NN–O bond. It should also be noted that the overall reaction of N_2O decomposition is exothermic ($\triangle H = -19.5$ kcal/mol).

There has been some discussion that metal particles might be much hotter than support materials during an exothermic reaction such as CO oxidation (22–24). Kember and Sheppard (22) estimated from infrared emission measurements that for a Pd/SiO_2 catalyst during CO oxidation at 300°C, there is at least 190°C temperature difference between the silica and metal components. On the other hand, Sharma *et al.* (23) concluded that the metal–support temperature gradients in a Pt/SiO_2 catalyst are small (<7°C) during CO oxidation. Matyi *et al.* (24) observed the local temperature rise (13–19°C) of an Fe/SiO_2 catalyst during CO hydrogenation. In our pulsed experiment using a small amount of N_2O (0.27 μmol), the temperature difference between the Rh particles and the USY support may be small. However, temporal and/or local heat dissipated from N_2O decomposition may facilitate the recombinative desorption of O_2. Alternatively, the hot O(a) atoms produced by N_2O decomposition may make a rapid exchange with the surrounding O(a) already present before O_2 desorption occurs. However, further discussion is needed to clarify how the energy transfer takes place on the surface.

CONCLUSIONS

Study of the dependence of oxygen coverage on pulsed N_2O decomposition revealed that activity increased with increasing coverage ($\theta_o > 0.5$) and that O_2 production started at $\theta_o \fallingdotseq 0.9$, and finally, steady-state activity was attained at high θ_o (>1.2). The O_2-TPD studies after N_2O or O_2 pretreatments suggest that oxygen species with weaker O–Rh bonds, which are desorbed below 700°C, play an important role in the high activity as well as the steady-state O_2 production in the catalytic N_2O decomposition. As revealed by the ^{18}O tracer study, however, O_2 desorption does not proceed via the ER mechanism (step [3]), but via the LH mechanism (step [2]) at low temperatures (220–240°C). On the other hand, the TPD study showed that O_2 desorption from the Rh/USY catalyst (in He) after the same O_2 treatment as in the isotopic study occurred at much higher temperatures (>500°C), which suggests reaction-assisted desorption of O_2 during N_2O decomposition.

REFERENCES

1. Kapteijn, F., Rodriguez-Mirasol, J., and Moulijn, J. A., *Appl. Catal. B* **9**, 25 (1996).
2. Li, Y., and Armor, J. N., *Appl. Catal. B* **1**, L21 (1992).
3. Oi, J., Obuchi, A., Bamwenda, G. R., Ogata, A., Yagita, H., Kushiyama, S., and Mizuno, K., *Appl. Catal. B* **12**, 277 (1997).
4. Leglise, J., Petunchi, J. O., and Hall, W. K., *J. Catal.* **86**, 392 (1984).
5. Centi, G., Dall'Olio, L., and Perathoner, S., *Appl. Catal. A* **194/195**, 79 (2000).
6. Winter, E. R. S., *J. Catal.* **15**, 144 (1969).
7. Lin, J., Chen, H. Y., Chen, L., Tan, K. L., and Zeng, H. C., *Appl. Surf. Sci.* **103**, 307 (1996).
8. Yuzaki, K., Yarimizu, T., Ito, S., and Kunimori, K., *Catal. Lett.* **47**, 173 (1997).
9. Yuzaki, K., Yarimizu, T., Aoyagi, K., Ito, S., and Kunimori, K., *Catal. Today* **45**, 129 (1998).
10. Yamashita, T., and Vannice, A., *J. Catal.* **161**, 254 (1996).
11. Root, T. W., Schmidt, L. D., and Fisher, G. B., *Surf. Sci.* **134**, 30 (1983).
12. Dandl, H., and Emig, G., *Appl. Catal. A* **168**, 261 (1998).
13. Caratzoulas, S., Jackson, B., and Persson, M., *J. Chem. Phys.* **107**, 6420 (1997).
14. Uetsuka, H., Aoyagi, K., Tanaka, S., Yuzaki, K., Ito, S., Kameoka, S., and Kunimori, K., *Catal. Lett.* **66**, 87 (2000).
15. Kunimori, K., Ikeda, Y., Soma, M., and Uchijima, T., *J. Catal.* **79**, 185 (1983).
16. Kunimori, K., Uchijima, T., Yamada, M., Matsumoto, H., Hattori, T., and Murakami, Y., *Appl. Catal.* **4**, 67 (1982).
17. Li, Y., and Bowker, M., *Surf. Sci.* **348**, 67 (1996).
18. Alfè, D., Rudolf, P., Kiskinova, M., and Rosei, R., *Chem. Phys. Lett.* **211**, 220 (1993).
19. Ozaki, A., "Isotopic Studies of Heterogeneous Catalysis." Kodansha, Tokyo, 1977.
20. Tanaka, S., Kameoka, S., Ito, S., and Kunimori, K., to be published.
21. Pedley, J. B., and Marshall, E. M., *J. Phys. Chem. Ref. Data* **12**, 967 (1984).
22. Kember, D. R., and Sheppard, N., *J. Chem. Soc. Faraday Trans. 2* **77**, 1321 (1981).
23. Sharma, S., Boecker, D., Maclay, G. J., and Gonzalez, R. D., *J. Catal.* **110**, 103 (1988).
24. Matyi, R. J., Butt J. B., and Schwartz, L. H., *J. Catal.* **91**, 185 (1985).